Proceedings of the Sixth International Conference on
Soft Computing, Machine Learning and Optimisation in
Civil, Structural and Environmental Engineering
Edited by: P. Iványi, J. Lógó and B.H.V. Topping
Civil-Comp Conferences, Volume 5, Paper 4.3
Civil-Comp Press, Edinburgh, United Kingdom, 2023
doi: 10.4203/ccc.5.4.3

Deep Learning Approach to Predict Acoustic Field in Transcranial Focused Ultrasound

M. Jang[1], M. Choi[1], I. Jeong[1], S.S Yoo[2], K. Yoon[3] and G. Noh[1]

[1]School of Mechanical Engineering, Korea University, Seoul, South Korea
[2]Department of Radiology, Brigham and Women's Hospital, Harvard Medical School, Boston, USA
[3]School of Mathematics and Computing, Yonsei University, Seoul, South Korea

Abstract

The distortion caused by the skull poses challenges in determining the intensity and focal position of ultrasound waves in transcranial focused ultrasound therapy. Computational simulations can address this but are limited by high computational costs. To overcome this, we propose a deep learning-based surrogate model that provides real-time generation of the focal position and distribution of ultrasound waves passing through the skull. The model is trained using data from computational simulations performed on multiple skulls, allowing it to reflect distortion characteristics and predict acoustic fields for any skull. The proposed model offers a promising solution for accurate and efficient real-time estimation of the intracranial acoustic field.

Keywords: deep learning, surrogate model, transcranial focused ultrasound, finite-difference time-domain, real-time

1 Introduction

Focused ultrasound (FUS) has been utilized in various disease treatments by noninvasively stimulating target tissues with locally concentrated mechanical energy within the biological tissue. Low-intensity transcranial FUS, in particular, allows for procedures such as brain stimulation [1,2] and drug delivery through blood-brain barrier opening [3,4] without tissue temperature changes [5], enabling research on a

range of conditions, including depression, Alzheimer's, neuropathic pain, disorders of consciousness following brain injury, and neuroregeneration after stroke.

Ultrasound exhibits characteristics of reflection and refraction when transmitted through biological tissues, particularly exhibiting severe distortion when passing through porous substances such as the skull. Computational ultrasound simulations [6] can consider distortion characteristics such as reflection and refraction, but real-time operation is limited due to the extremely high computational costs involved in predicting ultrasound within the skull.

The study proposes a deep-learning (DL) based model that offers real-time transcranial focused ultrasound (tFUS) acoustic field prediction for any skull data. The proposed universal tFUS model differs from the previous patient-specific model [7] in that it eliminates the need for individual patient training and incorporates skull data and transducer placement as input. To construct the DL-based model, a training dataset was generated using computational forward simulations for various skulls, and DL-based surrogate models were trained for estimating acoustic pressure value and acoustic field.

The study's main novelties are the proposed DL-guided universal tFUS model with real-time capability and the use of computational forward simulation-driven data to accurately estimate tFUS undergoing absorption, refraction, reflection, and attenuation. The proposed model offers a solution to the limitations of patient-specific models as it requires no further training for individual patients and has real-time operational capability.

2 Computational forward simulation for training data generation

Data for the computational ultrasound simulation consisted of a skull model, an ultrasound transducer model, and a model for the acoustic pressure field within the region of interest, as shown in Fig. 1. The skull model was generated from 16 three-dimensional CT scans with a resolution of 0.5 mm, and voxel data for the skull model were classified as water, diploic, and cortical bone based on Hounsfield Units. Thirteen of these skull models were used to generate training data, while the remaining three were used for testing and validation.

The ultrasound transducer model was set to a diameter of 96 mm, a curvature radius of 52 mm, and a focal length of 83 mm. The position and orientation of the transducer were based on the central coordinates of the exit surface. To generate training data, 6,318 samples were created by randomly varying the position and angle within a 20x20x20 mm region of motion for each skull model, and 729 samples were used for testing and validation.

The region of interest for ultrasound pressure field analysis within the skull was set to be 81x151x81 in size and located 50 mm from the central coordinates of the exit surface. The Westervelt-Lighthill [8,9,10] was used as the governing equation for the

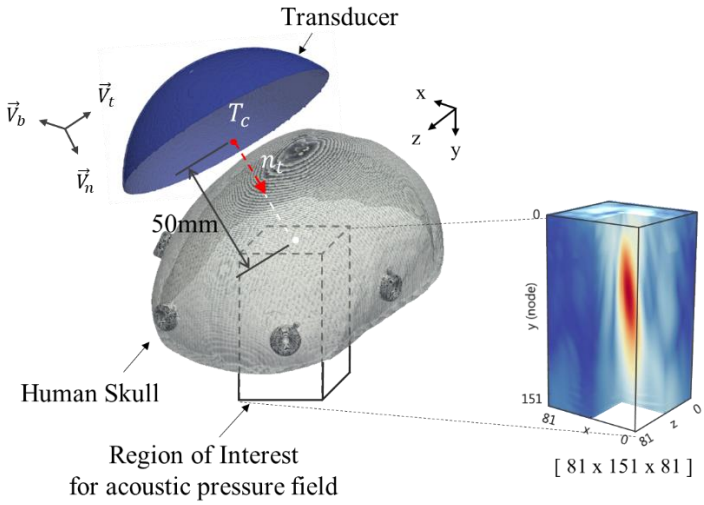

Figure 1: Schematics of modelling skull, a single-element transducer and acoustic pressure field in the region of interest.

analysis of the ultrasound pressure field within the region of interest, and the Finite-Difference Time-Domain (FDTD) method [6,11] was used for approximating the spatio-temporal partial derivatives. The acoustic pressure field, corresponding to the position of the skull and the ultrasound transducer, was analyzed with a time interval of $\Delta t = 0.1$ μs and 1200-time steps when an ultrasound of 250 kHz was applied.

3 Deep learning based surrogate model

We propose a deep learning-based surrogate model that predicts the acoustic field based on skull data and ultrasound transducer coordinates through three networks as shown in Fig. 2.

To efficiently train the network, we used a pre-trained VGG19 [12] to extract features of the skull. The VGG network is a CNN-based model trained on a large-scale visual database called ImageNet. It consists of 19 convolutional layers with 3x3 kernel sizes and 3 fully connected layers. We added a global average pooling layer to the feature extraction part composed of only convolutional layers, obtaining a feature matrix of size 315x512 from the calvaria data of size 315x400x400.

The acoustic distribution network (ADNet) takes the feature matrix of the skull as the first input and the position information of the transducer as the second input and outputs the acoustic pressure distribution. We used a convolutional autoencoder as the backbone network, consisting of 6 convolutional and transpose convolutional layers for both encoder and decoder. The input and output of the ADNet were normalized to -1 to 1. The objective function is as follows:

$$\mathcal{L}_{ADNet} = \arg\min \left(\|P - \bar{P}\|_2 \right) \quad (1)$$

where P and $\bar{P}$ denote the acoustic field generated by simulation (ground truth) and the ADNet, respectively.

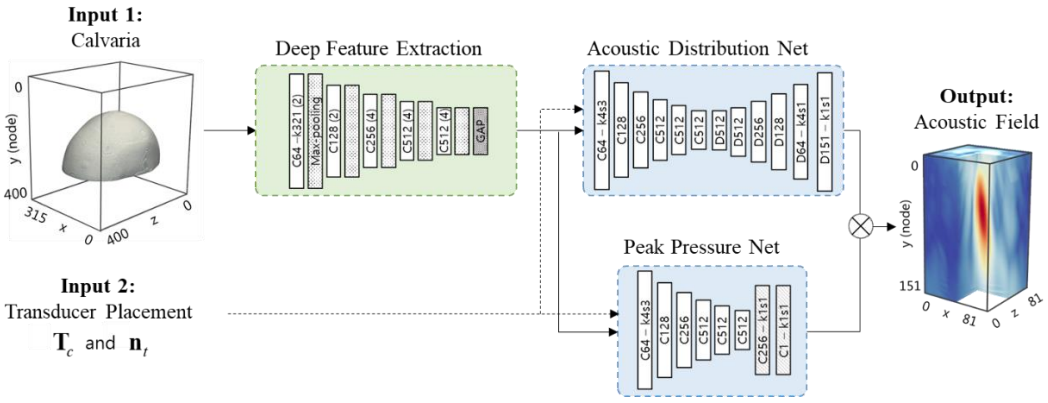

Figure 2: Schematic of our proposed a deep Learning-based surrogate model.

Finally, we introduced the peak pressure network (PPNet) to improve the accuracy of the estimated peak pressure of the acoustic focus. The PPNet takes the feature matrix of the skull and the position information of the transducer as input and outputs the peak pressure value of the acoustic focus. It has the same encoder structure as the ADNet, followed by 2 1x1 convolutional layers. The input and output were also normalized to -1 to 1. The objective function is as follows:

$$\mathcal{L}_{PPNet} = \text{argmin}\left(\left\| P_{peak} - \bar{P}_{peak} \right\|_2 \right) \tag{2}$$

where P_{peak} and $\bar{P}_{peak}$ denote peak pressure value obtained by simulation (ground truth) and the PPNet, respectively.

We used the BOHB algorithm [13] to search for the optimal hyperparameters that minimize the loss function of both networks. Each network was trained for 100 epochs with the optimal hyperparameters. All networks were trained using TensorFlow [14] in the computing environment of AMD Ryzen9-5950X CPU, NVIDIA GeForce 3090Ti-single GPU device, and 128.0-GB RAM.

4 Experimental validations

To evaluate the accuracy of the surrogate model, we conducted a tank experiment using skulls that were not used in the neural network training process. We measured a total of 15 acoustic fields in xy, yz, and xz planes by changing the position of 3 skulls in 5 ways. The experiment was performed in a water tank filled with degassed and distilled water, and virtual registration with the transducer and skull was performed using 2 and 4 markers, respectively.

To quantitatively evaluate the performance of the surrogate model, we measured the peak pressure ratio error (ΔPPR) at the focus, focal point error (ΔFP), Hausdorff distance (HD) between the boundaries of the two focus regions, and Dice similarity coefficient (DSC) to evaluate the similarity of the focus regions.

For each acoustic field, ΔPPR, ΔFP, HD, and DSC were defined as follows:

$$\Delta PPR = |R - \bar{R}|, \qquad R = \frac{P_{peak,\ skull}}{P_{peak,\ freefield}} \tag{3}$$

where R represents the ratio of the peak pressure after the transcranial application to the peak pressure measured without the skull. $\bar{R}$ represents the ratio to the peak pressure predicted by the PPNet.

$$\Delta FP = \sqrt{(c_x - \bar{c}_x)^2 + (c_y - \bar{c}_y)^2 + (c_z - \bar{c}_z)^2} \tag{4}$$

$$HD = max\big(h(F_b, \bar{F}_b),\ h(\bar{F}_b, F_b)\big)$$

$$h(F_b, \bar{F}_b) = \max_{f \in F_b} \min_{f' \in \bar{F}_b} ||f - f'||_2,$$

$$h(\bar{F}_b, F_b) = \max_{f' \in \bar{F}_b} \min_{f \in F_b} ||f' - f||_2 \tag{5}$$

$$DSC = \frac{2 * |F \cap \bar{F}|}{|F| + |\bar{F}|} \tag{6}$$

Where c_x, c_y, c_z denote the centroid location of the focal volume defined by FWHM, F and F_b denote the focal volume and the set of points corresponding to its boundary, respectively, and $\|f - f'\|$ denotes the Euclidean distance between points belonging to the boundary F or F_b . The upper bar in each symbol indicates the quantities obtained from the ADNet.

Table 1 summarizes the experimental validation results and computational performance of the proposed surrogate model for predicting acoustic fields. The simulation and surrogate model exhibited ΔPPR of 3.51 ± 0.81% and 3.94 ± 0.94%, respectively. Regarding the prediction of the acoustic distribution, the simulation demonstrated a ΔFP of 1.88 ± 0.37 mm, HD of 5.55 ± 0.84 mm, and DSC of 0.85 ± 0.03. On the other hand, the surrogate model showed a ΔFP of 2.46 ± 0.83 mm, HD of 5.90 ± 0.84 mm, and DSC of 0.81 ± 0.04. Examples of acoustic field predicted by the two approaches are presented in Fig. 3.

Regarding inference time, the simulation took 40 seconds to generate an acoustic field, while the surrogate model took 0.016 seconds. This highlights the potential of the proposed surrogate model to provide real-time acoustic field predictions with performance close to that of the simulation.

Method	ΔPPR [%]	ΔFP [mm]	HD [mm]	DSC	Inference time [s]
Simulation	3.51 ± 0.81	1.88 ± 0.37	5.55 ± 0.84	0.85 ± 0.03	40
Surrogate	3.94 ± 0.94	2.46 ± 0.83	5.90 ± 0.84	0.81 ± 0.04	0.016

Table 1: Experimental validation results of the computational simulation and deep learning-based surrogate model.

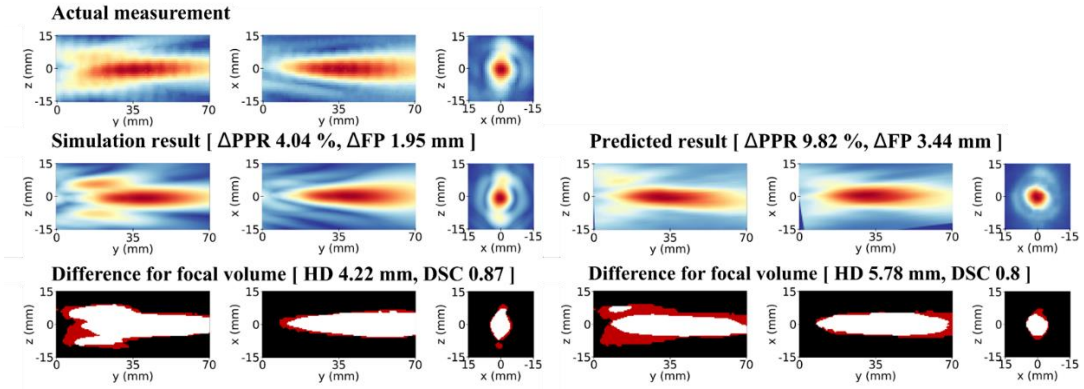

Figure 3: Comparative results with experimental data.

5 Conclusions

In this study, a DL-guided tFUS surrogate model was developed to estimate the acoustic energy transmitted from a single-element transducer for arbitrary skull data in real-time operations. The proposed model estimated the volumetric conformity of the acoustic field with approximately 85% accuracy in less than 5 ms. The findings suggest that the DL model has potential for use in the brain neuromodulation field, where rapid and precise visualization of the acoustic field is necessary.

However, the performance of the data-driven approach is dependent on the quantity and quality of the training dataset. the model was trained with a limited number of skull sets, and future studies should explore the effects of skull sample uncertainty. Furthermore, employing an advanced simulation model is expected to enhance the DL model's performance.

Future work will focus on constructing a model that estimates temperature distribution for acoustic focus to assess heat damage in the target region. These findings could have significant implications in the field of neuromodulation and improve the understanding of the acoustic field's effects on the brain.

Acknowledgment

This work was supported in part by the research project funded by the Institute of Information & communications Technology Planning & Evaluation (IITP) grant funded by the Korea government (MSIT) (2022-0-00824).

References

[1] C. Constans, P. Mateo, M. Tanter and J.F. Aubry, “Potential impact of thermal effects during ultrasonic neurostimulation: retrospective numerical estimation of temperature elevation in seven rodent setups”, Phys. Med. Biol., 63 (2), 025003, 2018,

[2] W. Lee, H. Kim, Y. Jung, I.U. Song, Y.A. Chung and S.S Yoo, “Image-guided transcranial focused ultrasound stimulates human primary somatosensory cortex”, Sci. Rep., 5 (1), 1-10, 2015.
[3] K. Yoon, et al., “Effects of sonication parameters on transcranial focused ultrasound brain stimulation in an ovine model”, PLoS One, 14 (10), e0224311, 2019.
[4] Y. Meng, S. Suppiah, S. Surendrakumar, L. Bigioni and N. Lipsman, “Low-intensity MR-guided focused ultrasound mediated disruption of the bloodbrain barrier for intracranial metastatic diseases”, Front. Oncol., 8, 338, 2018,
[5] K. Yoon, et al., “Blood–brain barrier opening in ovine model using image-guided transcranial focused ultrasound”, Ultrasound Med. Biol., 45, 9, 2391-2404, 2019.
[6] K. Yoon, W. Lee, P. Croce, A. Cammalleri and S.S Yoo, “Multi-resolution simulation of focused ultrasound propagation through ovine skull from a single-element transducer”, Phys. Med. Bio., 63 (10), 105001, 2018.
[7] M. Choi, M. Jang, S.S Yoo, G. Noh and K. Yoon, “Deep Neural Network for Navigation of a Single-Element Transducer During Transcranial Focused Ultrasound Therapy: Proof of Concept”, IEEE J. Biomed. Health Inform., 26 (11), 5653-5664, 2022.
[8] P.J. Westervelt, “Scattering of sound by sound”, J. Acoust. Soc. Am., 29 (2), 199-203, 1957.
[9] J. Lighthill, “Acoustic streaming”, J. Sound Vibr., 61 (3), 391-418, 1978.
[10] A. Kyriakou, E. Neufeld, B. Werner, G. Székely, N. Kuster, “Full-wave acoustic and thermal modeling of transcranial ultrasound propagation and investigation of skull-induced aberration correction techniques: a feasibility study”, Journal of Therapeutic Ultrasound, 3 (1), 1-18, 2015.
[11] G.F. Pinton, J. Dahl, S. Rosenzweig, G.E. Trahey, “A heterogeneous nonlinear attenuating full-wave model of ultrasound”, IEEE Trans. Ultrason. Ferroelectr. Freq. Control, 56 (3), 474-488, 2009.
[12] K. Simonyan, A. Zisserman, “Very deep convolutional networks for large-scale image recognition”, arXiv:1409.1556, 2014.
[13] S. Falkner, A. Klein, F. Hutter, “BOHB: Robust and efficient hyperparameter optimization at scale”, In International Conference on Machine Learning, PMLR, 1437-1446, 2018.
[14] M. Abadi, et al., “TensorFlow: a system for large-scale machine learning”, In 12th USENIX symposium on operating systems design and implementation (OSDI 16), 265-283, 2016.